Analysis of a Nuclear Reactor Support Structure

A. H. MARCHERTAS*
Argonne National Laboratory, Argonne, Ill.

AND

G. M. SMITH†
University of Nebraska, Lincoln, Nebr.

A general solution is presented for the deformation of a circular grid support structure, which consists of two parallel perforated plates positioned one above the other and interconnected by a large number of tubes. The solution is based on a modified shape function for a circular plate which may be subjected to any degree of edge restraint, ranging from fixed to simple supports. The Rayleigh-Ritz method is used in conjunction with the Lagrangian multiplier associated with the degree of edge restraint. The complexity introduced by the holes in the two plates is circumvented by the use of two equivalent solid plates. The solution is given in terms of a set of simultaneous algebraic equations with a general expression for the coefficients.

Nomenclature

a = outside radius of the plates, in.
A = undetermined coefficients of deflection function
B = total number of concentric regions in a plate
C = constant or coefficient
d = tube diameter, in.
D = $Eh^3/12(1 - \nu^2)$, flexural rigidity of plate, lb-in.
E = modulus of elasticity, lb/in.^{2}
f = intensity of uniformly distributed load, lb/in.^{2}
h = plate thickness, in.
i,j = indices referring to location of holes, tubes, or loads
I = $\pi(d_o^4 - d_i^4)/64$, tube moment of inertia, in.^{4}
k = constant indicating the degree of edge restraint; Eq. (5)
K_l,K_p,K_r = stress multipliers, given by O'Donnell and Langer[1]
l = distance between the plates, in.
m,n = indices of terms in deflection function; $m \neq 1, n \neq 1$
M = bending moment, lb-in.
N = maximum number of terms in series of deflection function
p,q = constants associated with edge restraint; Eq. (3)
P = individual loads, lb
r,θ,z = cylindrical coordinates of plates
s = distance between center lines of perforations, in.
t = minimum ligament width, in.
U = strain energy, in.-lb
V = potential energy due to external load, in.-lb
w = plate deflection, in.
W = total potential energy, in.-lb
x,y = coordinates of the tubes
β = See Eqs. grouped following (21)
δ = See Eqs. grouped following (21)
ζ = See Eqs. grouped following (21)
η = See Eq. (10)
λ = number of holes, tubes, or loads
ν = Poisson's ratio
ξ = See Eq. (6)
ρ = weight density, lb/in.^{3}
σ = unit stress, lb/in.^{2}
χ = Lagrangian multiplier

Subscripts

h = hole
i = inside
l = load
m,n = indices designating terms of a summation
o = outside
p = plate
r = radial
s = support
t = tube
θ = tangential

Received September 16, 1963; revision received February 28, 1964. This paper is based on a dissertation submitted by A. H. Marchertas to the University of Nebraska in partial fulfillment of the requirements for the degree of Doctor of Philosophy. The work was sponsored by the U. S. Atomic Energy Commission through the Argonne National Laboratory.

* Assistant Mechanical Engineer.
† Professor of Engineering Mechanics. Member AIAA.

Introduction

THE principal structural assembly within a nuclear reactor is the grid support structure for the nuclear fuel, safety, and control assemblies. A typical grid support structure is shown in Fig. 1. The perforations or holes are symmetrical with respect to the center of the plates and are arranged in an equilateral triangular pattern. Tubes extend through the holes and are rigidly connected to both plates. The fuel assemblies rest on the top plate of the structure, as shown in Fig. 2a. The total load consists of numerous concentrated loads of the fuel assemblies, weight of the tubes, and the distributed weight of the plates. For a nuclear rocket engine that is accelerating a vehicle in space, the loads on such a structure would, of course, depend upon the magnitude of acceleration.

Under load, the top and bottom plates deflect and the interconnecting tubes deform, as shown in Fig. 2a. Excessive deformation of the tubes could cause the protrusions of the fuel assemblies to contact the tube walls and bind during loading-unloading operations (see Fig. 2a). A substantial deformation of the plates during acceleration of the vehicle could tilt the fuel assemblies enough to affect the neutron flux of the reactor.‡ Furthermore, deflections will increase as temperature rises and may alter the nuclear reactivity characteristics significantly. Therefore, the operation and performance of a nuclear reactor depend to a considerable extent upon the rigidity of the grid support structure.

The purpose of this paper is to present a general solution for the analysis of the deflection and slope geometry and stress intensity of a nuclear reactor grid support structure. It is believed that the solution presented will be useful for reactors for nuclear-rocket engines. Since the grid structure would ordinarily be supported by the walls of the reactor vessel (see Fig. 1), the analysis should be sufficiently general to accommodate any degree of edge restraint.

‡ It is assumed in this analysis that the fuel assemblies are not restrained in any other way, so that no additional external moment is imparted to the tubes.

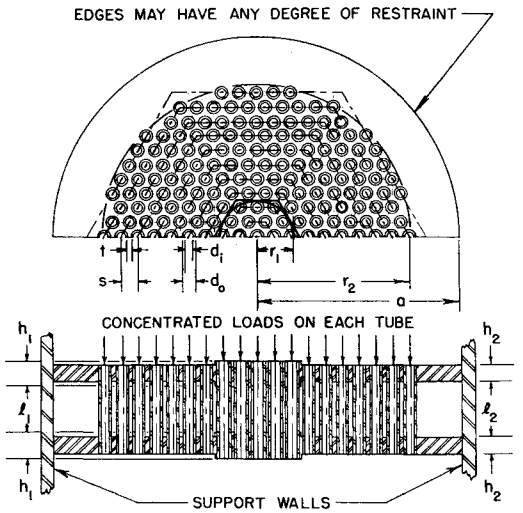

Fig. 1 Typical grid support structure of a nuclear reactor.

Basis for Analysis

The following assumptions are made:

1) The material of the structure obeys Hooke's Law.

2) Perforated plates of the grid structure can be treated as "equivalent solid plates" by using appropriate elastic constants. O'Donnell and Langer[1] have summarized the work done in the field of perforated plates, and the concept of an "equivalent plate" has gained rather wide acceptance.

3) Deformation of both plates of the structure is the same.

4) The deflection of the plates is axisymmetric.

5) Membrane stresses in the plates and axial stresses in the tubes are negligible.

6) An equivalent average moment may be assumed instead of the individual moments caused by the tubes.

The analysis is based on the general solution of a simplified problem. Since the number of loads on the structure is large, it is reasonable to base the solution on the deflection of a uniformly loaded circular plate. It is interesting to note that the general deflection (neglecting shear deflection) of the plate under a uniform load may be generalized to incorporate the complete range of edge restraints. This deflection may be concisely represented by the following expression:

$$w = \frac{fa^4}{64D}\left[\frac{\nu + 5 - 4k}{\nu + 1} - 2\,\frac{\nu + 3 - 2k}{\nu + 1}\left(\frac{r}{a}\right)^2 + \left(\frac{r}{a}\right)^4\right] \tag{1}$$

where the constant k depends on the degree of edge restraint and ranges from zero for simple supports to unity for fixed supports. The meaning of k may best be realized by observing the expressions of the radial edge moment and slope for the entire range of edge restraints; the moment may be shown to be in terms of k and the fixed edge moment ($k = 1$), and the slope in terms of k and the slope of a free edge ($k = 0$). The reations are as follows:

$$\left.\begin{aligned} M_r|_{r=a} &= kM_r|_{\substack{r=a\\k=1}} \\ \frac{dw}{dr}\bigg|_{r=a} &= (1-k)\,\frac{dw}{dr}\bigg|_{\substack{r=a\\k=0}} \end{aligned}\right\} \tag{2}$$

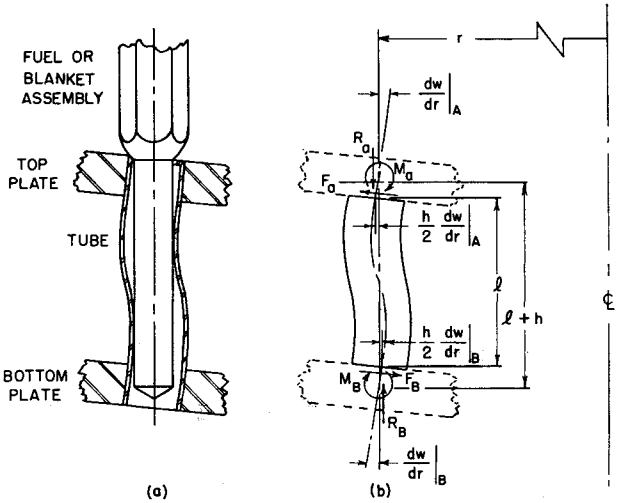

Fig. 2 Geometry and forces for interconnecting tubes.

Deflection Function

When the load on the plate is other than uniformly distributed but still symmetrical with respect to the center, the deflection expression of Eq. (1) must be modified. The modified deflection function or shape function may be taken in the form of the polynomial§

$$w = \sum_{n=0}^{\infty}\left[p_n - 2q_n\left(\frac{r}{a}\right)^2 + \left(\frac{r}{a}\right)^4\right]r^nA_n \qquad n \neq 1 \tag{3}$$

where

$$p_n = 1 + \frac{4(1-k)}{2n + \nu + 1} = \frac{2n + \nu + 5 - 4k}{2n + \nu + 1}$$

and

$$q_n = 1 + \frac{2(1-k)}{2n + \nu + 1} = \frac{2n + \nu + 3 - 2k}{2n + \nu + 1}$$

which derive their form from the two extreme boundary conditions. The A_n's are the undetermined coefficients which may be looked upon as the scaling factors of the shape function. The combined term r^nA_n has always the dimensions of deflection.

By direct differentiation of Eq. (3) and substitution into the expressions of plate theory, the radial moment and slope at the edge become

$$\left.\begin{aligned} M_r|_{r=a} &= -\frac{8Dk}{a^2}\sum_{n=0}^{\infty} a^nA_n \\ \frac{dw}{dr}\bigg|_{r=a} &= -\frac{8(1-k)}{a}\sum_{n=0}^{\infty}\frac{a^nA_n}{2n + \nu + 1} \end{aligned}\right\} \tag{4}$$

It may be observed from Eqs. (4) that now the moment and slope at the edge are functions of A_n, which may be either positive or negative. The sign of the moment and slope, however, is established by physical considerations of the problem. Thus, in order to ascertain the correct sign, it becomes necessary to choose the coefficients such that the condition

$$M_r|_{r=a} = kM_r|_{\substack{r=a\\k=1}} \tag{5}$$

is always satisfied. It is interesting to note that satisfying the geometric boundary condition

$$\frac{dw}{dr}\bigg|_{r=a} = (1-k)\,\frac{dw}{dr}\bigg|_{\substack{r=a\\k=0}}$$

in place of the moment restriction is insufficient. In other words, the geometric boundary conditions of deflection and

§ It should be noted that the term $n = 1$ is excluded from the series because it involves a discontinuity in subsequent calculations.

slope alone are unable to control the sign of the radial moment at the edge.

Potential Energy of the System

For the purpose of evaluating the undetermined coefficients, it is necessary to express the total potential energy of the system in terms of A_n. This potential energy consists of several parts, namely, strain energy of the plates, tubes, supports, and the potential energy due to the external loads. The separate component parts of the potential energy are discussed in the succeeding sections.

Strain Energy of Plates

Since bending alone is considered in the deformation, the strain energy stored in a circular plate[2] of radius a is

$$U_p = \frac{D}{2}\int_0^{2\pi}\int_0^a \xi\, dr\, d\theta \tag{6}$$

where

$$\xi = \left[\left(\frac{d^2w}{dr^2}\right)^2 + \frac{1}{r^2}\left(\frac{dw}{dr}\right)^2 + \frac{2\nu}{r}\left(\frac{d^2w}{dr^2}\right)\left(\frac{dw}{dr}\right)\right]r$$

In the design of the reactor support structures it is practically impossible to use plates that are uniform in thickness or are solid throughout. It is often necessary to make the plate thinner in some places and/or make it perforated in others. To accommodate this possibility the plate area is divided into several concentric zones, as shown in Fig. 1. In this case the strain energy of the plate becomes

$$U_p = \frac{1}{2}\int_0^{2\pi}\left[\sum_{b=1}^{B} D_b \int_{r_{b-1}}^{r_b} \xi_b\, dr\right] d\theta \qquad r_B = a \tag{7}$$

where each subscripted symbol refers to an appropriate effective elastic constant (D_b,ν_b) in the zone circumscribed by r_b; B is the total number of such zones.

Performing the indicated mathematical operations, the strain energy of both plates may be written in terms of the undetermined coefficients as follows:

$$U_p = \sum_{m=0}^{\infty}\sum_{n=0}^{\infty} C_{mn}' A_m A_n \tag{8}$$

where $m \neq 1$, $n \neq 1$, and $m \leq n$ in Eq. (8) *and all equations that follow*. It will be shown in a subsequent section that C_{mn}' is expressed in terms of the summation indices m and n, the geometrical constants and the elastic properties of the structure.

Strain Energy of Tubes

The strain energy due to bending of the tubes is

$$U_t = \frac{6E_tI(l+h)^2}{l^3}\sum_{i,j}^{\lambda_t}\left(\frac{dw}{dr}\right)_{i,j}^2 \tag{9}$$

where the indices i and j refer to any convenient planar coordinate system. However, Eq. (9) does not indicate the location of the tubes with respect to the plates. In order to correct this discrepancy, the expression is revised as follows:

$$U_t = \eta\int_0^{2\pi}\int_0^a \left(\frac{dw}{dr}\right)^2 r\, dr\, d\theta \tag{10}$$

where $\eta = 6\lambda_t E_t I(l+h)^2/\pi a^2 l^3$. This revised expression implies a uniform variation of the tube strain energy over the region between the plates instead of the algebraic energy sum of the individual tubes.

It would not be unusual to conceive of a structure with different sizes of tubes. For this reason the area of the plates again may be imagined to be divided into several concentric regions with different sizes of tubes. In this case the modified strain energy of the tubes becomes

$$U_t = \int_0^{2\pi}\left[\sum_{b=1}^{B}\eta_b\int_{r_{b-1}}^{r_b}\left(\frac{dw}{dr}\right)^2 r\, dr\right] d\theta \qquad r_B = a \tag{11}$$

and the subscripts refer to elastic constants in the appropriate regions of the plates. The strain energy of the tubes, as in the case of the plates, may be expressed in the form

$$U_t = \sum_{m=0}^{\infty}\sum_{n=0}^{\infty} C_{mn}'' A_m A_n \tag{12}$$

Strain Energy of Supports

The strain energy stored in the supports is proportional to the product of the radial moment and slope at the edge of the plates. This energy becomes

$$U_s = \frac{1}{2}\left[2\pi a M_r|_{r=a}\right]\left.\frac{dw}{dr}\right|_{r=a} \tag{13}$$

or

$$U_s = \sum_{m=0}^{\infty}\sum_{n=0}^{\infty} C_{mn}''' A_m A_n \tag{14}$$

Potential Energy of External Loads

The change in potential energy due to the external load is the sum of the products of the individual loads and their corresponding deflections:

$$V = -\sum_{i,j}^{\lambda_l} P_{i,j} w_{i,j} = -\sum_{n=0}^{\infty} C_n A_n \tag{15}$$

where the last expression is in terms of undetermined coefficients A_n.

Final Analysis

The total potential energy W of the system may be combined into a single expression as follows:

$$W = \sum_{m=0}^{\infty}\sum_{n=0}^{\infty} C_{mn} A_m A_n - \sum_{m=0}^{\infty} C_m A_m \tag{16}$$

where $C_{mn} = C_{mn}' + C_{mn}'' + C_{mn}'''$. This potential energy in the case of the two extreme boundary conditions ($k = 0$ and $k = 1$) may be directly subjected to the requirements of the principle of minimum potential energy; i.e., $\partial W/\partial A_m = 0$. For $0 < k < 1$, in addition to minimizing W, the moment restriction given by Eq. (5) must also be satisfied. By introducing the first of Eqs. (4), the moment condition represented by Eq. (5) may be more conveniently written as

$$\sum_{n=0}^{\infty} a^n A_n = -\frac{a^2}{8D_B} M_r\Big|_{\substack{r=a\\k=1}} = C_N' \tag{17}$$

In order to include the additional condition into the analysis, a mathematical tool known as the Lagrangian multiplier method may be utilized. This method results in the modified energy expression

$$\overline{W} = \sum_{m=0}^{\infty}\sum_{n=0}^{\infty} C_{mn} A_m A_n + \chi\sum_{m=0}^{\infty} a^m A_m - \sum_{m=0}^{\infty} C_m A_m \tag{18}$$

where χ is the Lagrangian multiplier. The modified energy equation is subject to the same requirements as in the previous case: $\partial\overline{W}/\partial A_m = 0$. The result of minimizing the total potential energy expression with respect to a particular A_m yields

$$\sum_{n=0}^{\infty} C_{mn} A_n + a^m\chi = C_m \qquad (m = 0,2,3,\ldots,\infty) \tag{19}$$

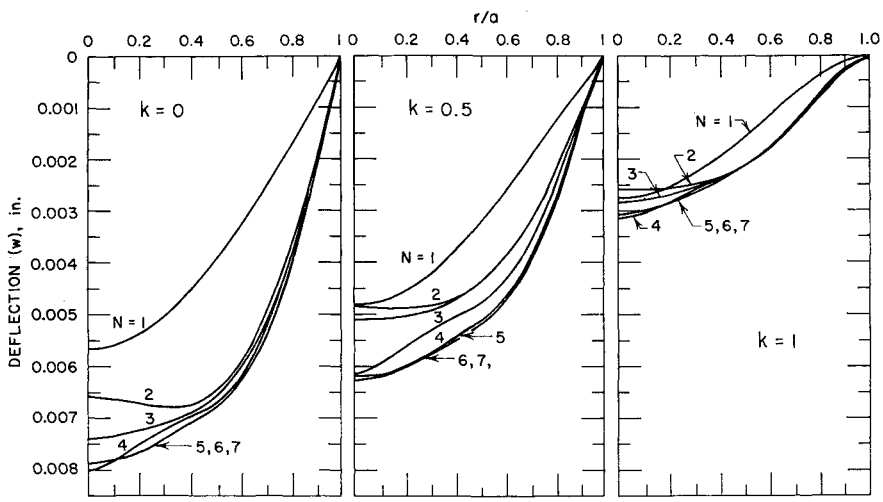

Fig. 3 Pictorial convergence of deflection function.

The evaluation of the coefficients A_n may now be accomplished by the solution of the simultaneous algebraic equations (17) and (19), where, in Eq. (19):

$$C_m = \sum_{i,j}^{\lambda t} P_{i,j}(r_{i,j})^m \left[p_m - 2q_m \left(\frac{r}{a}\right)^2_{i,j} + \left(\frac{r}{a}\right)^4_{i,j} \right] \quad (20)$$

$$C_{mn} = 4\pi \Bigg\{ p_m p_n mn \sum_{b=1}^{B} [D_b(\delta_1 + \nu_b)\beta_1 - \zeta_b\beta_2/\phi_2] -$$

$$2p_m q_n m(n+2) \sum_{b=1}^{B} [D_b(\delta_2 + \nu_b)\beta_2 + \zeta_b\beta_3/\phi_3] -$$

$$2q_m p_n (m+2)n \sum_{b=1}^{B} [D_b(\delta_3 + \nu_b)\beta_2 + \zeta_b\beta_3/\phi_3] +$$

$$p_m m(n+4) \sum_{b=1}^{B} [D_b(\delta_4 + \nu_b)\beta_3 + \zeta_b\beta_4/\phi_4] +$$

$$4q_m q_n (m+2)(n+2) \sum_{b=1}^{B} [D_b(\delta_5 + \nu_b)\beta_3 + \zeta_b\beta_4/\phi_4] +$$

$$p_n(m+4)n \sum_{b=1}^{B} [D_b(\delta_6 + \nu_b)\beta_3 + \zeta_b\beta_4/\phi_4] -$$

$$2q_m(m+2)(n+4) \sum_{b=1}^{B} [D_b(\delta_7 + \nu_b)\beta_4 + \zeta_b\beta_5/\phi_5] -$$

$$2q_n(m+4)(n+2) \sum_{b=1}^{B} [D_b(\delta_8 + \nu_b)\beta_4 + \zeta_b\beta_5/\phi_5] +$$

$$(m+4)(n+4) \sum_{b=1}^{B} [D_b(\delta_9 + \nu_b)\beta_5 + \zeta_b\beta_6/\phi_6] \Bigg\} +$$

$$128\pi k(1-k) D_B (a)^{\phi_1} \left(\frac{1}{2m + \nu_B + 1} + \frac{1}{2n + \nu_B + 1} \right)$$

$$r_B = a \quad (21)$$

where

$$\phi_c = m + n + 2(c-2) \qquad c = 1,2 \ldots 6$$

$$\beta_c = [(r_b)^{\phi_c} - (r_{b-1})^{\phi_c})]a^{2(c-1)} \qquad c = 1,2 \ldots 6$$

$$\delta_1 = [1 + (m-1)(n-1)]/\phi_1$$

$$\delta_2 = [1 + (m-1)(n+1)]/\phi_2$$

$$\delta_3 = [1 + (m+1)(n-1)]/\phi_2$$

$$\delta_4 = [1 + (m-1)(n+3)]/\phi_3$$

$$\delta_5 = [1 + (m+1)(n+1)]/\phi_3$$

$$\delta_6 = [1 + (m+3)(n-1)]/\phi_3$$

$$\delta_7 = [1 + (m+1)(n+3)]/\phi_4$$

$$\delta_8 = [1 + (m+3)(n+1)]/\phi_4$$

$$\delta_9 = [1 + (m+3)(n+3)]/\phi_5$$

$$\zeta_b = a^2\eta_b/[(r_b)^2 - (r_{b-1})^2]$$

For practical purposes it is frequently sufficiently accurate to deal with a finite number of equations. Unfortunately, the number of terms N needed in the series for a given problem cannot be predicted in advance. The more complex the load distribution and the tube arrangement, the greater the number of terms. For the selection of the appropriate N it becomes essential to follow through a number of solutions, each successive time increasing the equations by 1. This type of solution for a required quantity possesses the property of convergence. If the magnitude of at least two successive solutions are very close to each other, then the number of terms needed in the deflection series is assumed to be sufficient.

Once N is determined and the corresponding coefficients A_m are evaluated, Eq. (3) provides the deflection of the plates. It is important to note that, because of the presence of the stiffening tubes in the structure, the maximum deflection does not necessarily take place in the center of the plates. The easiest way to ascertain this maximum would be by plotting $w = f(r)$.

The configuration of the tubes may be determined from elementary beam theory. Hence, the deflection of a tube

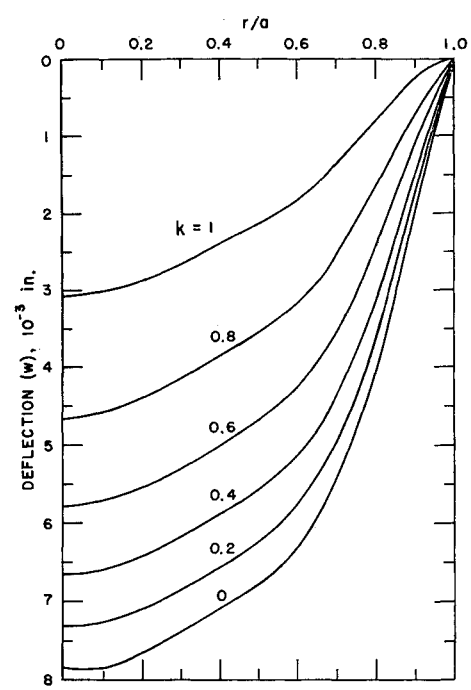

Fig. 4 Resultant deflections for various values of edge restraint.

in terms of the slope of the plate at the location of the tube is found to be

$$y = g(x)(dw/dr) \tag{22}$$

where

$$g(x) = (1/4l^3)[8(l + h)x^3 - 12(l + h)^2x^2 + 2(2l^3 + 6l^2h + 9lh^2 + 3h^3)x - h^2(l + h)(3l + h)]$$

and dw/dr is found by differentiating Eq. (3). It should be recalled again that if reference is made to any particular region of the plates, the appropriate physical constants (ν, E, D, l, h, d_0, d_i) for that region should be used. The maximum deflection of the tubes takes place wherever $g(x)$ and dw/dr have their maximum values. Since the maximum value of $g(x)$ is independent of the tube location, the maximum tube deflection becomes

$$y_{\max} = \frac{3^{1/2}}{18}\left[\frac{(l + 3h)^3}{l + h}\right]^{1/2}\left(\frac{dw}{dx}\right)_{\max} \tag{23}$$

where $(dw/dr)_{\max}$ is the maximum angular deflection at the end of the most deformed tube. The stress at the outside diameter of the tube is

$$\sigma_t = \frac{3E_t d_0(l + h)}{l^3}(l + h - 2x)\frac{dw}{dr} \tag{24}$$

and the corresponding maximum stress is

$$(\sigma_t)_{\max} = \frac{6E_t d_0(l + h)}{l^2}\left(\frac{dw}{dr}\right)_{\max} \tag{25}$$

The radial and tangential stress in the solid and also the equivalent portions of the plates are derived from the conventional deflection relationships yielding

$$\sigma_r = -\frac{6D}{h^2}\sum_{n=0}^{N}\left[p_n n(n - 1 + \nu) - 2q_n(n + 2)(n + 1 + \nu)\left(\frac{r}{a}\right)^2 + (n + 4)(n + 3 + \nu)\left(\frac{r}{a}\right)^4\right] r^{n-2}A_n \tag{26}$$

$$\sigma_\theta = -\frac{6D}{h^2}\sum_{n=0}^{N}\left\{p_n n[\nu(n - 1) + 1] - 2q_n(n + 2)[\nu(n + 1) + 1]\left(\frac{r}{a}\right)^2 + (n + 4)[\nu(n + 3) + 1]\left(\frac{r}{a}\right)^4\right\} r^{n-2}A_n \tag{27}$$

Where the stresses in the equivalent portion of the plate are known, the pertinent stresses in the perforated region may also be approximated. These stresses are

$$\begin{aligned}\sigma_{ls} &= K_l\frac{s}{l}|\sigma_1| \\ \sigma_{ps} &= K_p\sigma_1 + f \\ \sigma_{rs} &= K_r\sigma_{\text{rim}} + f\end{aligned} \tag{28}$$

which are the ligament, peak, and rim stresses, respectively; $\sigma_1 = \sigma_r$ or σ_θ, whichever has the greater numerical value. The values of the coefficients K_l, K_p, K_r are given in Ref. 1.

The procedure developed in this paper is applicable both to hand and computer (IBM-704) calculations. The solution of the given problem is considered obtained whenever the unknown coefficients A_n of the deflection function are evaluated. This is accomplished by constructing the needed number of simultaneous equations and directly solving for the A_n's. A single expression is presented in the analysis for evaluating all of the constants of the coefficient matrix and another expression for the terms of the constant vector.

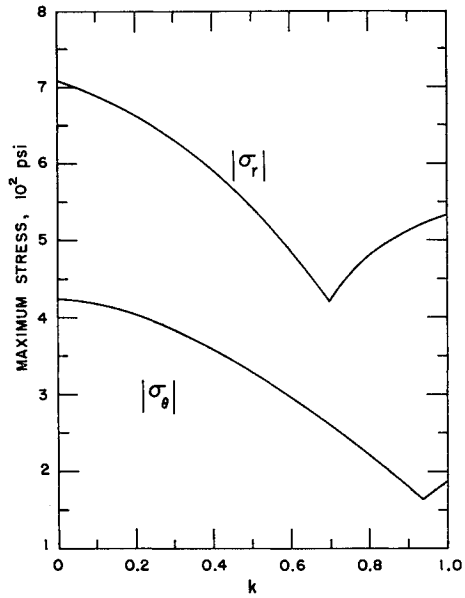

Fig. 5 Maximum radial σ_r and tangential σ_θ stresses in homogeneous plates.

Example Problem

Practical use of this analysis was made by predicting the deflections and pertinent stresses of the Experimental Breeder Reactor II¶ grid structure. Because of limited space the physical dimensions of the grid structure will not be given here. This is just as well, for the qualitative aspects of the solution, more than the quantitative, illuminate the veracity of the analysis.

The results of the example solution (obtained with a FORTRAN II program of an IBM-704) are illustrated by

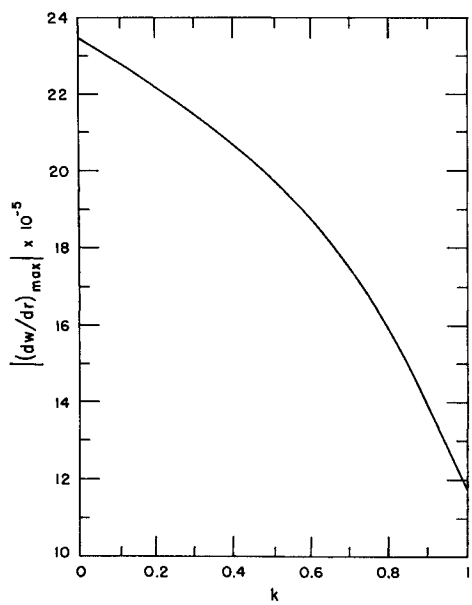

Fig. 6 Maximum angular deformation of tube.

¶ This is one of a series of breeder reactors designed and operated by the Argonne National Laboratory (ANL) under the auspices of the U. S. Atomic Energy Commission. An experimental check of the analysis given in this paper is presently under way at ANL and will be published as an ANL report.

Figs. 3–6. Figure 3 shows the gradual decrease in computed plate deflection as the number of terms taken into account in the series increases. The effect of edge restraint k may also be observed by comparing the parts of Fig. 3, and resultant deflection for the entire range of edge restraint is given in Fig. 4. It may be pointed out that the reinforcing tubes are arranged in an annular region ($0.34 \leq r/a \leq 0.71$) of the plates, the presence of which is exhibited by the flat portion (Fig. 4) of the deflection curves.

Figure 5 shows the maximum radial and tangential stresses in the equivalent homogeneous plate of the grid structure without reference to their location. These values may be used in conjunction with Eq. (26) to predict the important stresses in the perforated plates. For low values of k, it was found that the maximum stress takes place at the outer edge of the distributed tubes ($r/a \simeq 0.71$), and for values of k close to unity, the predominant stresses occur at the edges of the plates. It is interesting to note that, from the point of view of strength, the most efficient design takes place at some intermediate edge restraint; in this particular case $k = 0.7$. Of course, the exact fixity at the edge, established by the analysis, is very difficult to realize in actual practice. Nevertheless, the fixed edge condition is recommended in the actual design of the grid structure, for it never can be fully attained. When the rigidity of the edges is reduced by the structural imperfections, then the actual edge restraint will approach $k = 0.7$. In this way the deformation of the structure will also be kept at a minimum.

The stresses and deflections in the tubes depend on the slope to which the tubes are subjected. Hence, Fig. 6 gives the necessary information for obtaining the maximum tube deflections for all values of edge restraint.

Results of this example and other solutions infer to the authors that on occasion certain simplifications may be made without seriously impairing the accuracy of the solution. The equivalent circular approximation, for instance, could be used for the hexagonal load distribution without any noticeable discrepancy. This simplification may amount to a considerable saving of labor if hand computations are used. Still a greater simplification to the true load distribution is the assumption of the equivalent uniformly distributed load. This assumption is less accurate than that of the circular load distribution but could be used where the variation of load is small.

References

[1] O'Donnell, W. T. and Langer, B. F., "Design of perforated plates," Trans. ASME (Am. Soc. Mech. Eng.) Ser. B: J. Eng. Ind. **84**, no. 3, 307–320 (1962).

[2] Timoshenko, S. P. and Woinowsky-Krieger, S., *Theory of Plates and Shells* (McGraw-Hill Book Co., Inc., New York, 1959), pp. 342–347.